Conceptual Validation of a Prototype Passive Microwave Snow Water Equivalent Retrieval Algorithm for Tundra Environments

PETER TOOSE,[1] CHRIS DERKSEN,[1] ANDREW REES,[2] ARVIDS SILIS[1],
WALTER STRAPP[1], ANNE WALKER[1]

ABSTRACT

Measured brightness temperatures (T_B) of dry snow at vertically polarized 37 GHz decreases linearly with increasing snow water equivalent (SWE) until a threshold value is reached, after which a reversal in this relationship occurs and T_B begins to increase. This slope reversal has been observed in deep taiga and alpine snowpacks when SWE exceeds approximately 180 mm. A slope reversal of 37V T_B has also been observed for the tundra over several winters using AMSR-E satellite data. A prototype tundra specific algorithm has been developed that retrieves SWE across tundra regions by exploiting cumulative absolute changes in spaceborne 37V T_B's through the snow cover season. Accurate and extensive in situ snow observations coupled with T_B's measured over an entire winter are needed to properly validate the new prototype SWE algorithm. Unfortunately, data with these characteristics do not exist for tundra regions. However, detailed snow measurements and coincident high resolution airborne T_B's were acquired at three different study sites across the Canadian sub-arctic in 2008 during International Polar Year (IPY). These short-term measurements were not meant to characterize the seasonal evolution of the tundra snowpack. However, due to the extreme variability in snow characteristics over the three months covered by these campaigns, they can be suitable as a proxy for the range in SWE and T_B expected to be measured over the course of an entire winter season across the tundra. Evidence of the T_B versus SWE slope reversal using the high resolution airborne data occurs between 120mm-130mm of SWE, after which T_B's begin to increase with SWE providing conceptual validation that the seasonal reversal in observed AMSR-E satellite 37V T_B is likely due to increases in SWE.

INTRODUCTION

Accurate, long-term, sub-Arctic snow cover information is required for climatological, hydrological, and numerical modeling applications in northern regions. However, information on sub-Arctic tundra snow cover across Canada is limited by a sparse conventional observing network that is often not representative of the surrounding conditions, and has a strong coastal bias. Satellite passive microwave snow monitoring is a viable alternative. Operational methods for estimating SWE with passive microwave data in prairie and boreal forest environments are presently in use in Canada. In its simplest form, these SWE algorithms are based on the difference in T_B between vertically polarized 37 GHz and 19 GHz measurements. In shallow snow (SWE <150 mm) the T_B difference has a linear relationship with SWE: the greater the difference, the

[1]Atmospheric Science and Technology Directorate, Environment Canada, 4905 Dufferin St. Toronto, Ontario, M3H 5T4.
[2] Nipissing University, Department of Geography, North Bay, Ontario, P1B 8L7.

higher the SWE estimate. No passive microwave algorithms exist, however, for high latitude regions. Attempts to extend the application of any existing passive microwave SWE algorithms into the data sparse Canadian tundra environment have struggled with access to reliable and extensive snow observations for validation purposes. Those studies that have made use of locally collected field measurements have reported a consistent underestimation of SWE by conventional algorithms (Boudreau and Rouse, 1994; Derksen et al., 2005; Rees et al., 2005). This underestimation has in part, been linked to the unique radiometric properties of lake ice (Derksen et al, 2009; Toose, 2007). The lake ice influence evolves over the course of the winter as the thickness of the ice and snow on ice changes, and is dependent on the wavelength of the measured T_B. The 19 GHz emissions from sub-ice liquid water penetrate through thick tundra ice because of its longer wavelength and therefore can influence T_B's measured over frozen lakes throughout the winter. The 19 GHz emissions from sub-ice liquid water results in a much smaller difference in T_B when using 37V – 19V algorithms, leading to erroneously low SWE estimates. Another contributing factor to SWE underestimation is likely due to the relationship between the measured T_B of dry snow at 37V and SWE. The 37V T_B decreases linearly with increasing SWE until a threshold value is reached, after which a reversal in this relationship occurs and T_B's begin to increase with increasing SWE. The 37V T_B slope reversal has been documented in taiga and alpine regions where high SWE values (>200 mm) are common (Mätzler et al., 1982; De Sève et al., 1997). When this slope reversal occurs, algorithms based on a simple linear relationship will always underestimate SWE.

A 37V T_B slope reversal has been observed over the course of several years using Advanced Microwave Sounding Radiometer for EOS (AMSR-E) satellite data over the Canadian tundra environment. Figure 1 compares the AMSR-E 37V T_B's with coincident years of Baker Lake, NT (64° 18'N 96° 4.8' W) snow course data, illustrating the 37V slope reversal link with increasing SWE.

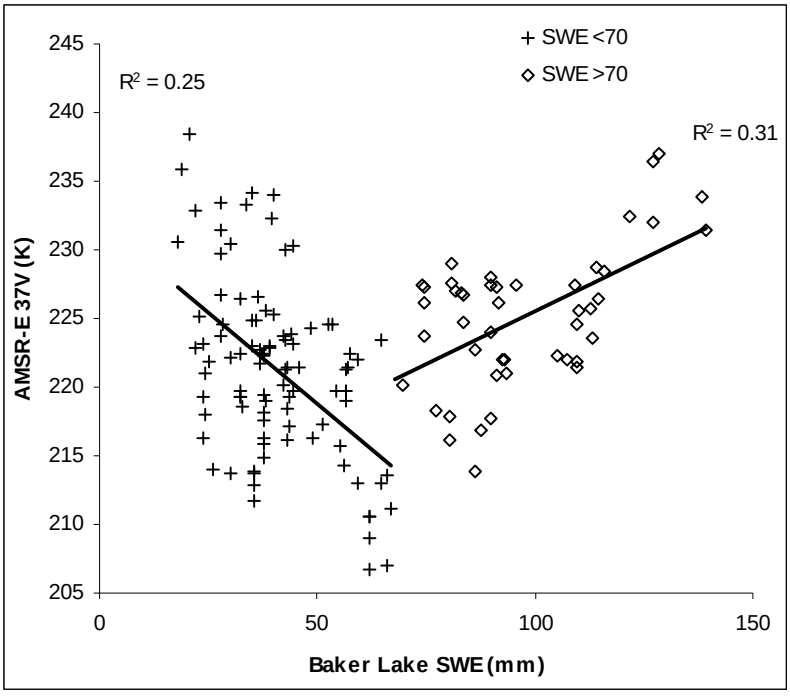

Figure 1 2003-2007 AMSR-E 37V T_B's versus Baker Lake, NT, SWE measurements

The r^2 values are strongest when the inflection point of the slope reversal is defined at 70 mm of SWE. The SWE values below 70 mm exhibit a negative association (r^2=0.25) with the 37V T_B's, while the SWE values above 70 mm exhibit a positive association (r^2 = 0.31) with the 37V T_B's.

Based on these findings, a prototype 37V single frequency SWE algorithm was developed at Environment Canada (presently not published). The algorithm takes into account the cumulative absolute change in 37V GHz T_B which is computed at a pentad interval from a January 1 start date to the end of April. Using in situ measurements from across the Canadian sub-Arctic, a greater (lower) cumulative change in 37V was significantly related to greater (lower) ground measured SWE (r^2=0.67). Cumulative change in 37V was only weakly correlated with lake fraction: monthly r^2 values calculated for January through April 2003-2007 were largely less than 0.2. These results illustrate that this algorithm is largely insensitive to the influence of lakes and takes into account the slope reversal issue. Unfortunately, there are limited numbers of extensive, full season surface SWE measurements available over the Canadian tundra to independently validate this new algorithm. However, during International Polar Year in 2008, three tundra study sites were visited across the Canadian sub-arctic. Each of these field campaigns were not seasonal in nature, but instead were conducted over relatively short (one to three week) time periods between February and April. They involved the collection of extremely detailed snow measurements and coincident high resolution passive microwave airborne data acquisitions.

The main purpose of these field campaigns was to take a snap-shot of the current snow conditions during the period of study, not to observe the seasonal evolution of the snowpack. However, due to the heterogeneous nature of tundra snow, a wide range of T_B's and coincident snow conditions (similar to what one would expect to find over the course of a single season) were encountered. The IPY dataset is not a continuous time series, and so is not suitable for testing the single frequency prototype algorithm, but it can be used to test the soundness of the primary algorithm concept that a slope reversal in 37V T_B is evident using high resolution passive microwave airborne data collected across the Canadian sub-arctic. The presence of a 37V GHz slope reversal in this trans-tundra dataset would indicate that this reversal is most likely linked to increasing SWE magnitude and not some other seasonal artifact, providing evidence that a single frequency time series algorithm that exploits this relationship is conceptually sound.

STUDY AREAS:

Three separate field campaigns took place in 2008 during IPY supported research in and around (1) Puvirnituq, Quebec (February 18th to March 5th); (2) the Tundra Ecosystem Research Station, Daring Lake, NT (April 1st to April 10th); and (3) Trail Valley Creek near Inuvik, NT (April 3rd to April 16th). The location of each study site is illustrated in Figure 2. Daring Lake and Puvirnituq are located well north of the treeline in a Canadian shield tundra region with complex terrain including boulder fields and exposed bedrock. Trail Valley Creek near Inuvik is characterized by gently rolling hills of shrub tundra with incised creek and river valleys. This site was located close to the forest/tundra transition zone, with small stands of coniferous trees found in valleys and on sheltered slopes.

DATA AND METHODS:

GPS coordinates and detailed measurements of snow depth, SWE, snow density, snow stratigraphy and snow grain size were recorded by observers on the ground. Standard methods were used to measure snow stratigraphy, density, and SWE. A total of ~80 km of continuous snow depth measurements were recorded between all sub-Arctic study sites by using a self-recording snow depth probe (Magna Probe) linked to a GPS. Grain size was measured using a stereo-microscope and comparator card. Passive microwave airborne T_B's were acquired at high resolutions (80m x ~100m) from dual-polarized 6.9, 19.35 and 37 GHz microwave radiometers mounted on board the National Research Council of Canada's (NRC) Twin Otter aircraft.

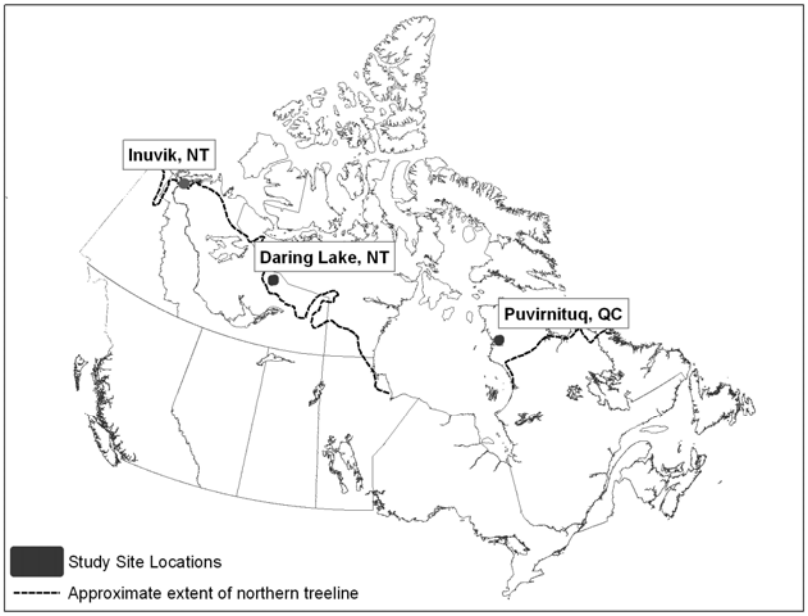

Figure 2 Trans-tundra study site locations.

Each individual T_B was geo-tagged with latitude and longitude coordinates as the aircraft flew along hundreds of kilometres of flight lines during all three field campaigns. The aircraft GPS navigation system and handheld GPS units carried by the snow surveyors were used to co-locate the ground measurement sites and the acquisition of the airborne T_B's. The snow surveyors used a set of handheld Garmin GPS Map 60C units. These units are WAAS enabled allowing for positional accuracy of better than 3 meters 95 percent of the time (Garmin™, 2009). WAAS signal reception is ideal for open land and marine applications (Garmin™, 2009), and therefore these units are aptly suited for the flat and expansive tundra environment.

Geographic Information System (GIS) software was used to assess the accuracy of the co-location of the georeferenced snow survey and airborne data by calculating the approximate extent of the instantaneous field of view (IFOV) for each airborne T_B and then overlaying these airborne footprints on the ground data to identify regions of overlap. The airborne radiometer's IFOV is dependent on the aircraft's ground speed and altitude, as well as the radiometer's beamwidth, view angle, and integration time. The radiometer's data acquisition system automatically calculates the latitude and longitude coordinates for each T_B taking into account the height above ground and the radiometer's beamwidth and view angle, including the aircraft's pitch, roll and yaw. The T_B's are tagged with GPS coordinates at the initial onset of the radiometer integration time, representing the location on the surface of the earth where the radiometers begin acquiring data. They stop acquiring data after one second, and then the cycle is repeated. The distance between adjacent T_B coordinates is dependent on the speed of the aircraft, which is typically flown at 110 nautical mph during science flights, or approximately 60m/sec on the ground. The relative consistency of the aircraft speed results in typical IFOV size fluctuations in the along-track axis of less than 10 meters for most flights. The collection of very high resolution airborne data, such as in the measurements acquired for this analysis, results in a longer IFOV extent in the along-track axis due to the forward momentum of the aircraft and the one second integration time. This lengthening of the radiometer footprint in the along-track axis is an important consideration for this study because the total number of snow measurements that fall within the radiometer's IFOV will vary depending on the size of the IFOV. This effect becomes less important when working with coarser resolution airborne data because the extent of the IFOV becomes larger than the distance traveled during the one second integration time and therefore adjacent T_B's are heavily overlapped, leading to an over-sampled dataset.

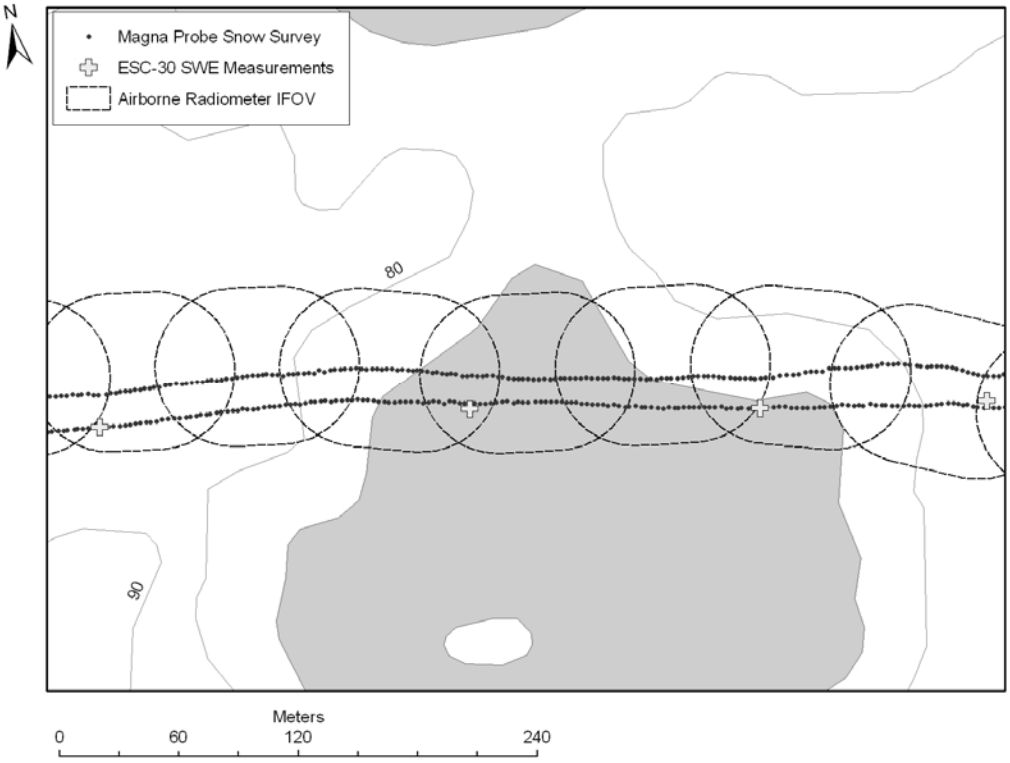

Figure 3 Airborne 37V GHz T_B's IFOVs and aligned coincident snow measurements.

Figure 3 shows a visual representation of the snow survey and airborne data collected during the Puvirnituq field campaign combined using ArcGIS™ software. The snow depth transect transitions from open tundra on to a small pond and then back on to land. The black dashed oblong shapes approximate the IFOV of the high resolution airborne radiometers (80m x ~100m). The two lines of points passing through the IFOVs represent two side-by-side snow depth transects, and each individual point is a snow depth measurement recorded using the GPS Magna Probes. The cross symbols represent the location of the manual ESC-30 SWE measurements recorded to obtain the bulk snowpack density and water equivalent. Average land cover specific snow densities measured at each study site location were calculated based on these ESC-30 measurements and available Landsat land cover classifications. These land cover specific snow densities were used to estimate a snow water equivalent value for each snow depth measurement based on the land cover class it was measured in.

In reality, the precise co-location of the surface snow measurements within the airborne T_B footprint does not always occur. This is largely due to errors in navigation by both the aircraft flight crew and the snow surveyors. In Puvirnituq, 18.5km of continuous snow measurements were recorded parallel to approximately 350 airborne T_B's, with 62 percent of them falling within the IFOV of those T_B's. At the Daring Lake study location 33km of continuous snow measurements were recorded parallel to approximately 625 airborne T_B's, with again 62 percent of them being measured within the IFOV. At the Trail Valley Creek study location near Inuvik 28km of continuous snow measurements were recorded parallel to 1100 T_B's with only 35 percent of all snow measurements being co-located within the airborne T_B's IFOV. Figure 4 illustrates the common misalignment that occurred between the airborne and snow measurements during all three IPY field campaigns.

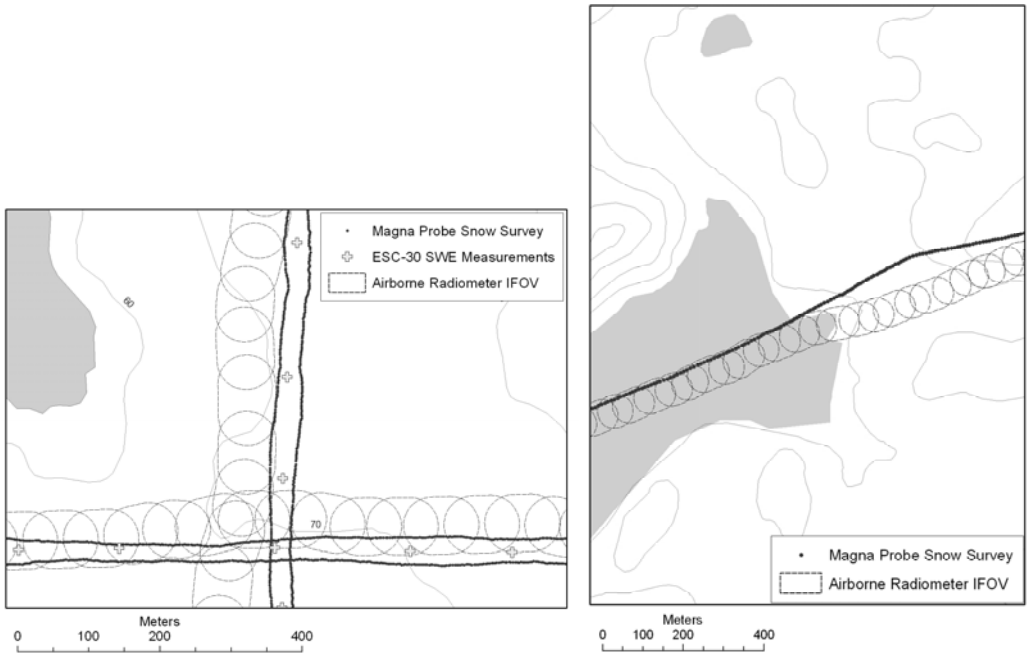

Figure 4 Airborne 37V GHz T_B's IFOVs and misaligned coincident snow measurements.

In total 995 T_B's from all three trans-tundra study site locations had 11,909 coincident SWE measurements within the IFOV's of the radiometers. However, this includes T_B's which potentially only had a single snow measurement and/or had measurements at the very edge of an IFOV boundary. Therefore, to ensure that each T_B was compared to an adequate and representative number of SWE measurements a simple filtering process was used. The first stage of filtering eliminated all T_B's with snow measurements at the margins of the IFOV that might not have been representative of the snowpack within the IFOV itself. This was accomplished by using the GIS software to select only those T_B's with snow measurements at least 10 m inside the boundary of the IFOV, resulting in a total of 882 T_B's with 9,066 coincident SWE measurements.

The second step of the filtering process involved selecting only those T_B's with a large enough number of snow measurements to capture the local scale variability in SWE that is common for the heterogeneous tundra snowpack. Therefore, only those airborne T_B's with at least 10 SWE measurements within the IFOV were selected for this analysis. A sample size of at least 10 snow measurements was considered large enough to not be overly affected by one or two non-representative measurements within the IFOV. This selection process resulted in a total of 694 T_B's with 8,630 coincident SWE measurements.

The final stage of filtering involved removing several outliers identified in the scatter plot of the 37V airborne T_B's versus the Magna Probe SWE measurements. In total 11 T_B's from the Puvirnituq and Daring Lake sites were removed based on their placement in the scatter plot leaving 683 T_B's and approximately 8,400 coincident snow measurements for analysis. The 11 outliers typically had mid to high SWE values with very high 37V T_B's, and were located in lake/land transition zones (10 out of 11 outliers). Higher SWE values tend to be found along lake/land transition zones, concentrated in tight narrow bands around the lake margins. When the airborne radiometer's IFOV crosses these narrow bands of high SWE the majority of the footprint is still sensing the shallow snowpack on top of the lake ice, resulting in high 37V T_B's. However, when the snow surveyors cross the narrow band, several very deep snow measurements can easily skew the average SWE values too high for those T_B's resulting in obvious outlying measurements in the scatter plot. The final results of the 37V airborne T_B's versus estimated SWE from the Magna Probe depth measurements are provided in figure 5.

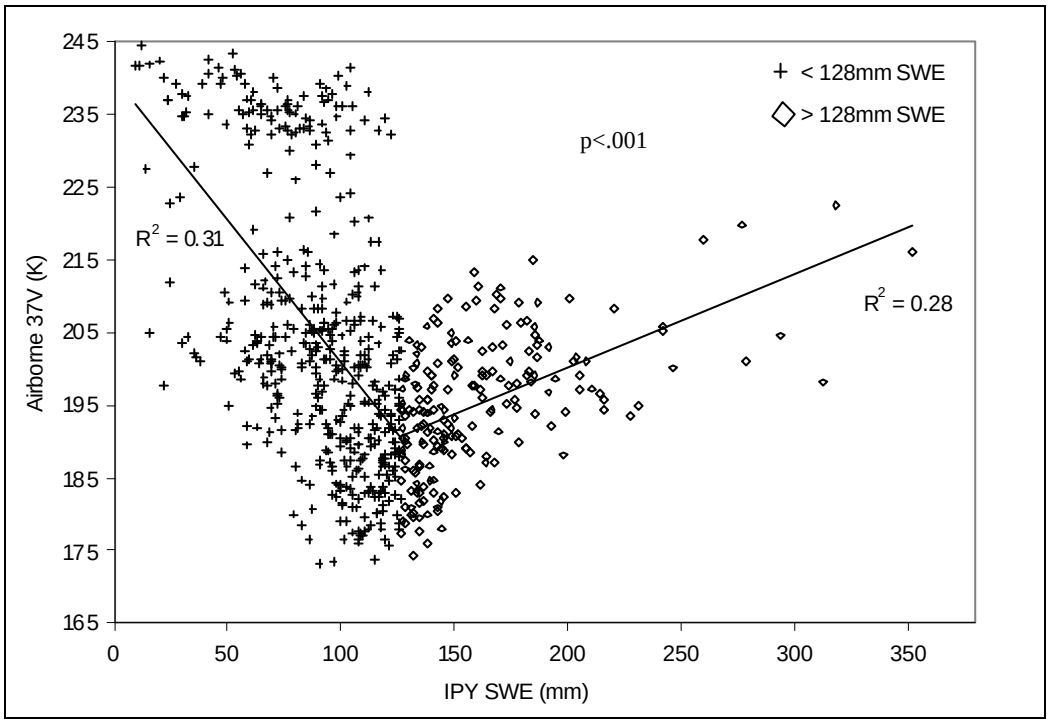

Figure 5 Airborne 37V T_B's versus snow measurements from all three IPY study sites.

RESULTS AND DISCUSSION:

A slope reversal in the relationship between the 37V passive microwave airborne data and estimated SWE from the Magna Probe depth measurements is evident in this trans-tundra dataset. Figure 5 illustrates that the r^2 values (significant $p < .001$) are strongest when the inflection point of the slope reversal is defined at 128 mm of SWE. The SWE values below 128 mm exhibit a negative relationship ($r^2 = 0.31$) with the 37V T_B's, while the SWE values above 128 mm exhibit a positive relationship ($r^2 = 0.28$) with the 37V T_B's. The scatter plot in figure 5 also highlights the most commonly measured SWE values, within the range of 80mm to 160mm, which is the magnitude that one would expect to find in a tundra environment during mid-to-late winter (February-April). It also shows that the sheer size of our snow measurement and airborne data sample allowed us to capture enough measurements at either end of the spectrum to illustrate the 37V slope reversal. The moderate r^2 values of the slopes are quite similar to those observed at the satellite scale in figure 1, while the figure 5 scatter plot better highlights the extreme variability in SWE and T_B commonly found in this environment.

Although the slope reversal is evident with the airborne data, the magnitude at which point the reversal occurs is different than what was observed with the AMSR-E satellite data and Baker Lake, NT, snow course data (128 mm versus 70 mm). Both of these inflection points are less than the approximate 180mm which was previously documented in alpine and taiga environments by Mätzler et al., 1982 and De Sève et al., 1997, respectively, and the taiga value of 140 mm identified by Derksen (2008). The difference between the Baker Lake and trans-tundra inflection points could be related to a snow measurement sample size issue or it could be a sensor resolution issue between airborne and satellite data. Unlike the relatively homogeneous mid-to-late season airborne measurements, the AMSR-E footprint that covers Baker Lake is composed of approximately 30% lake fraction. This sub-grid heterogeneity will have a seasonally evolving influence on T_B throughout the winter that did not influence the airborne data. In addition, the Baker Lake snow course covers a relatively localized area, and is being compared to coarse resolution passive microwave satellite data, (re-sampled to 25km EASE-Grid), which covers a

much larger region. The Baker Lake data may be underestimating the surrounding tundra SWE, so in reality the inflection point might be much closer to the 128mm, but this cannot be confirmed without extensive local snow measurements which currently do not exist.

CONCLUSIONS:

A slope reversal in 37V T_B versus SWE was observed for the tundra over several winters using AMSR-E satellite data and Baker Lake, NT snow course data. The slope reversal was used to develop a prototype tundra specific algorithm that bases its SWE estimates on the cumulative absolute changes in 37V T_B throughout the snow cover season. Unfortunately, validation of this algorithm using reliable and extensive snow observation for high latitude regions is difficult due a limited observation network. However, detailed snow measurements and coincident high resolution airborne T_B's were acquired at three different study sites across the Canadian sub-arctic during IPY. These short-term measurements are suitable as a proxy for the range in SWE and T_B expected to be measured over the course of an entire winter season across the tundra. The 37V slope reversal was evident when the high resolution airborne data and IPY SWE measurements, were compared, with the inflection point occurring between 120mm-130mm of SWE. The magnitude at which point the reversal occurred was different than that observed using satellite data, but the presence of a slope reversal in this trans-tundra dataset provides reasonable evidence that the observed slope reversal in the AMSR-E satellite T_B measurements, can be linked to changes in SWE magnitude and not some other seasonal artifact, such as changes to snowpack structure or grain size.

ACKNOWLEDGMENTS

Thanks to all of the snow surveyors involved in the collection of this IPY dataset, including Erin Thompson and Dave McNichol from Environment Canada, Scott Ketcheson from Wilfrid Laurier University, and Alec Casey from the University of Waterloo. Thanks to all the National Research Council's Twin Otter aircraft flight crew and pilots and Environment Canada flight personnel for the long days required to acquire the airborne data and calibrate the radiometers. A special thanks to members of the Nunavik Arctic Survival Training Centre in Puvirnituq, QC for assistance with our field campaign logistics and Wilfrid Laurier's Cold Regions Research Centre and the University of Waterloo's Interdisciplinary Centre on Climate Change for lending us the necessary equipment for completing this work.

REFERENCES

Boudreau LD. Rouse WR. 1994. Algorithm testing of passive microwave monitoring of snow water equivalent in a tundra environment. *Report Contract Number KM040-2-9008*, Atmospheric Environment Service, Environment Canada, 70 pp.

Derksen, C. M. Sturm, GE. Liston, J. Holmgren, H. Huntington, A. Silis, D. Solie. 2009. Northwest Territories and Nunavut snow characteristics from a subarctic traverse: implications for passive microwave remote sensing. *Journal of Hydrometeorology* **10**: pp 448-463.

Derksen, C. 2008. The contribution of AMSR-E 18.7 and 10.7 GHz measurements to improved boreal forest snow water equivalent retrievals. *Remote Sensing of Environment* **112**: 2700-2709.

Derksen, C. A. Walker, and B. Goodison. 2005. Evaluation of passive microwave snow water equivalent retrievals across the boreal forest / tundra transition of western Canada. *Remote Sensing of Environment.***96(3-4):** pp 315-327.

De Sève, D. M. Bernier, JP. Fortin, and A. Walker. 1997. Preliminary analysis of snow microwave radiometry using the SSM/I passive microwave data: the case of La Grande River watershed (Quebec). *Annals of Glaciology* **25**: pp 353-261.

Garmin™. About GPS – What is WAAS? [*Article*]. Available at: http://www8.garmin.com/aboutGPS/waas.html [Accessed July 29th 2009].

Mätzler, C. E. Schanda, and W. Good. 1982. Towards the definition of optimum sensor specifications for microwave remote sensing of snow. *IEEE Transactions on Geoscience and Remote Sensing* GE-20 (**1**): pp 57-66.

Rees, A., M. English, C. Derksen and A. Walker. 2005. Assessing snowpack water equivalent distribution in an open tundra environment using various scales of passive microwave data. *62nd Eastern Snow Conference Proceedings*, Waterloo, Ontario, Canada. pp 229-233.

Toose, P. 2007. The influence of snow cover variability and tundra lakes on passive microwave remote sensing of late winter snow water equivalent in the Hudson Bay lowlands, Masters Thesis. University of Waterloo, Waterloo, Ontario.